

Birth, interactions, and evolution over topography of solitons in Serre-Green-Naghdi model

Qingcheng Fu¹, Alexander Kurganov^{1,2,3}, Mingye Na¹ and Vladimir Zeitlin⁴ ²†

¹Department of Mathematics, Southern University of Science and Technology, Shenzhen, 518055, China

²Shenzhen International Center for Mathematics, Southern University of Science and Technology, Shenzhen, 518055, China

³Guangdong Provincial Key Laboratory of Computational Science and Material Design, Southern University of Science and Technology, Shenzhen, 518055, China

⁴Laboratory of Dynamical Meteorology, Sorbonne University, Ecole Normale Supérieure, CNRS, 75005 Paris, France

(Received xx; revised xx; accepted xx)

New evidence of surprising robustness of solitary-wave solutions of the Serre-Green-Naghdi (SGN) equations is presented on the basis of high-resolution numerical simulations conducted using a novel well-balanced finite-volume method. SGN solitons exhibit a striking resemblance with their celebrated Korteweg-deVries (KdV) counterparts. Co-moving solitons are shown to exit intact from double and triple collisions with a remarkably small wave-wake residual. The counter-propagating solitons experiencing frontal collisions and solitons hitting a wall, non-existing in KdV case configurations, are shown to also recover, but with a much larger than in co-moving case residual, confirming with higher precision the results known in the literature. Multiple SGN solitons emerging from localized initial conditions are exhibited, and it is demonstrated that SGN solitons survive hitting localized topographic obstacles, and generate secondary solitons when they encounter a rising escarpment.

Key words: Serre-Green-Naghdi equations, solitons, multi-soliton solutions, bottom topography

1. Introduction

Serre-Green-Naghdi (SGN) equations is a generalization of the classical shallow-water equations obtained by relaxing the hydrostatic approximation in the standard derivation, cf. e.g. (Dellar & Salmon 2005). The model was first derived by Serre (1953) and then rediscovered by Su & Gardner (1969) in the one-dimensional configuration relevant to the present study, although without topography. The emphasis in the later work Green & Naghdi (1976) was on two-dimensional motions in the presence of topography. Finite-amplitude steady-moving solutions in a form of periodic cnoidal waves, and solitary waves as their limiting form, are known in the SGN system starting from (Serre 1953; Su & Gardner 1969). It is also well-known (Su & Gardner 1969), that the celebrated Korteweg-deVries (KdV) equation arises as an asymptotic limit of the SGN equations in the case of unidirectional weakly nonlinear waves. The KdV equation possesses exact solutions in the form of cnoidal waves and solitons, which were known for a long time. Yet one of the most striking properties of the KdV equation is that it possesses also exact multi-soliton solutions. (We will place ourselves from now on in the

† Email address for correspondence: zeitlin@lmd.ens.fr

framework of decaying boundary conditions, and will not discuss periodic waves). These multi-soliton solutions were first discovered numerically in a landmark paper by Zabusky & Kruskal (1965), and their existence triggered the studies of complete integrability of the KdV equation, which was later successfully proved. In fact, any localized initial condition for the KdV equation is being transformed into a sequence of solitons of different amplitudes and speeds. Let us recall that Zabusky and Kruskal observed a striking behavior of the KdV solitons, which they used to initialize numerical simulations: the solitons passed one through another recovering their initial shape after multiple collisions.

A natural idea to make numerical experiments *à la* Zabusky & Kruskal (1965) with SGN solitons, in order to compare the behavior of corresponding multi-soliton configurations, arises in this context. The SGN solitons are routinely used for testing numerical methods for the SGN equations, e.g. (Le Métayer *et al.* 2010; Pearce & Esler 2010; Bonneton *et al.* 2011), while existing studies of their collisions are sparse (Mirie & Su 1982; Dutykh *et al.* 2013; Mitsotakis *et al.* 2017), limited to collisions of pairs of SGN solitons, and mostly in the frontal configuration which is motivated by experimental studies, e.g. (Cheng & Yeh 2014), and is impossible for KdV solitons. A study in the aforementioned spirit is by Craig *et al.* (2006), where strong resemblance with the behavior of KdV solitons was emphasized, but still on the basis of pairwise soliton collisions, and in the framework of the full Euler equations (see a corpus of literature on theoretical, experimental, and numerical investigations on collisions of soliton solutions of Euler equations therein)—not for the SGN model. On the other hand, laboratory experiments on soliton interactions with localized topographic obstacles, and early numerical simulations (Seabra-Santos *et al.* 1987) show that solitons survive collisions with bumps and escarpments, and produce a secondary trailing soliton-like structure in the latter case

In this paper, we present numerical experiments on collisions of SGN solitons and their interactions with topography. The results obtained with the help of a novel well-balanced high-resolution numerical method, confirm the surprising robustness of SGN solitons. We study not only double, but also triple-soliton configurations, and show that co-moving SGN solitons basically reproduce the behavior of KdV solitons. The SGN solitons, unlike the KdV ones, can propagate in both directions, so we also study frontal collisions, and collisions with a vertical wall. We also present results of experiments on interaction of SGN solitons with topographic obstacles, giving additional evidence of their robustness. Finally, we show that localized initial conditions give rise to one- or multi-soliton configurations, depending on their shape. The bulk of our results supports the conjecture that multi-soliton configurations are attracting quasi-exact solutions of the SGN equations.

2. SGN equations, their soliton solutions, and key points of the numerical method

The SGN equations in one spatial dimension x read as

$$\begin{cases} h_t + uh_x + hu_x = 0, \\ u_t + uu_x + g(h+b)_x + \frac{1}{3h} \left(h^2 \mathcal{D}^2 \left(h + \frac{3}{2}b \right) \right)_x + b_x \mathcal{D}^2 \left(\frac{1}{2}h + b \right) = 0, \end{cases} \quad (2.1)$$

where $h(x, t)$ is the thickness of the fluid layer, $u(x, t)$ is its velocity, $b(x)$ is the bottom topography, g is the acceleration due to gravity, and $\mathcal{D} := \frac{\partial}{\partial t} + u \frac{\partial}{\partial x}$ is the material time derivative. Localized exact solutions of (2.1) with $b \equiv 0$, solitary waves or solitons, having a maximal amplitude h_{\max} , and moving with a constant speed c on the background of unperturbed depth h_∞ , are given by

(e.g. (Le Métayer *et al.* 2010)):

$$\begin{cases} h(x, t) = \widehat{h}(x - ct) = h_\infty + (h_{\max} - h_\infty) \operatorname{sech}^2 \left(\sqrt{\frac{3(h_{\max} - h_\infty)}{h_{\max} h_\infty^2}} \frac{(x - ct)}{2} \right), \\ u(x, t) = \widehat{u}(x - ct) = c \left(1 - \frac{h_\infty}{\widehat{h}(x - ct)} \right), \quad c = \pm \sqrt{h_{\max}}. \end{cases} \quad (2.2)$$

These solutions can propagate with the same speed $\sqrt{h_{\max}}$ both left- and rightwards. It is important that they decay exponentially, so if several solitons are initially placed sufficiently far from each other, the overlapping of their tails is exponentially small. Such configurations will be used for initialization in §3.

The simulations presented in §3 have been conducted using a novel flux globalization based well-balanced central-upwind scheme. We only sketch the main idea of its construction here, the full details will be presented elsewhere. We first reformulate the system (2.1) in the following quasi-conservative form:

$$\begin{cases} h_t + q_x = 0, \\ Q_t + K_x = 0, \end{cases}$$

where $q := hu$, $Q := q(1 + h_x b_x + \frac{1}{2}hb_{xx} + b_x^2) - \frac{1}{3}(h^3u_x)_x$, and K is a global flux:

$$K := hu^2 + \frac{g}{2}h^2 - \frac{h}{3}[hq_x u_x + (qhu_x)_x] + \frac{1}{2}(q^2 b_x)_x + qub_x^2 + \int^x [ghb_x + qb_{xx}(\frac{1}{2}hu_x - ub_x)] dx.$$

We then design a well-balanced scheme, which is capable of exactly preserving certain physically relevant steady states satisfying

$$q \equiv \text{Const}, \quad K \equiv \text{Const}, \quad (2.3)$$

at the discrete level. Note that formula (2.3) contains both “moving-water” $q \neq 0$ and “still-water” $q \equiv 0$ steady states (2.3).

We construct our well-balanced scheme along the lines of (Chertock *et al.* 2018a,b; Cheng *et al.* 2019; Kurganov *et al.* 2020; Chertock *et al.* 2022): we reconstruct the equilibrium quantities q and K instead of h and q , and then recover the point values of h by solving the corresponding nonlinear equations. In additions, as the evolved quantities are h and Q , we compute q at the end of each time evolution step by solving the corresponding tridiagonal linear systems. In order to reduce the numerical dissipation present in the central-upwind scheme and to increase the efficiency of the resulting scheme, we implement the moving framework approach from (Kliakhandler & Kurganov 2009).

We emphasize that the soliton solution (2.2) in the reference frame moving with its speed is a “still-water” steady state, and the numerical scheme is capable of *exactly* preserve it provided the initial conditions are “well-prepared”. Such preparation, however, requires solving for h at given q and K , which is rather complicated and will not be done below. We, however, take advantage of the fact that the well-balanced property of the scheme guarantees that small numerical oscillations due to the initial discretization errors do not amplified in time and also rapidly decay when the mesh is refined, which we have checked. If the code is initialized with (2.2), the soliton keeps moving while maintaining its initial shape for as long as we follow it (not shown), but zooming reveals small-amplitude oscillations at its rear. They are, however, rapidly decreasing with increasing resolution, as shown in Fig. 1. The amplitude of these oscillations should be compared with the amplitude of the soliton $h_{\max} = 12.1$. We also stress that while the total energy of the system is not perfectly conserved during the simulations, a typical overall decrease of the total energy normalized by its initial value is $\sim 10^{-6}$.

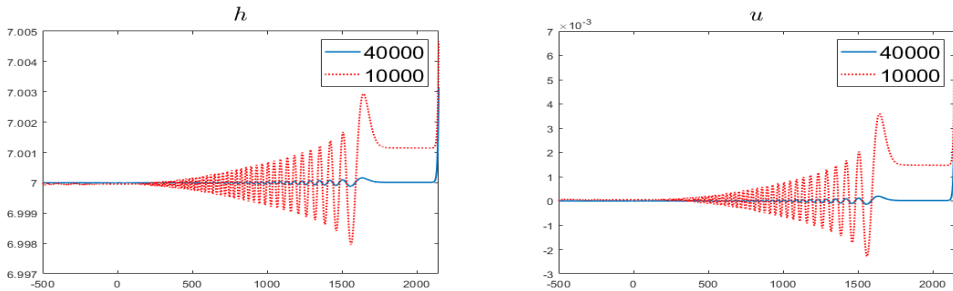


FIGURE 1. Zoom of numerical oscillations in h (left) and u (right) at the rear of the soliton at two resolutions with 40000 and 10000 cells in the computational domain $[-2500, 2500]$.

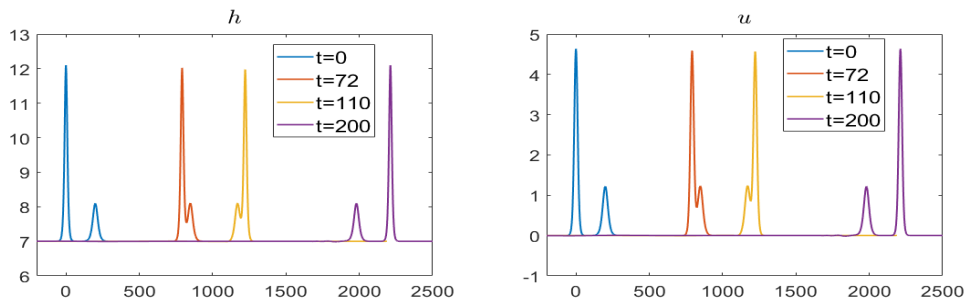


FIGURE 2. Snapshots of a collision of two co-moving solitons with maximum heights, respectively $h_{max} = 12.1, 8.1$ for two solitons at $H = 7$. Left (right) panel: height (velocity) field.

3. Results of numerical simulations

3.1. Soliton collisions

3.1.1. Collisions of co-moving solitons

We start by a two-soliton encounter by placing a higher amplitude (faster) soliton behind a lower amplitude (slower) soliton, with the same sign of velocity, and at a sufficient distance, in order to have a negligible overlapping, and let them go. As follows from Fig. 2, the rear soliton passes through the front one and rapidly recovers its form after collision. The collision produces a rapidly dispersed wave packet of small amplitude gravity waves left behind the solitons. Both solitons engaged in the collision preserve their form quasi-exactly, as follows from Fig. 4. The amplitude difference, not visible at the scale of the figure, is less than half per-cent point-wise, both in height and velocity (not shown). The L_2 norms of initial and final state are, respectively, 21.6138, and 21.6131. The residual represents a small-amplitude wave wake, which is not of numerical origin, as its amplitude does not decrease with increasing resolution, cf. Fig. 3. The existence of the wave-wake was proven theoretically by an asymptotic analysis for the same process in the framework of full Euler equations, cf. (Byatt-Smith 1988) and references therein, so there is no doubt that it is of physical origin. During the collision process the slower soliton accelerates, while the faster soliton decelerates, as follows from the comparison of their positions at the end of the simulation with those each of them would have at the same moment of time if propagating freely by itself.

We then examine three-soliton interactions. If we place three solitons of increasing amplitude one behind another with a lesser distance between the two front solitons, we observe sequential pairwise collisions of the kind presented above. The solitons pass through each other recovering their form after collisions, which produce each time emission of rapidly dispersing packets of

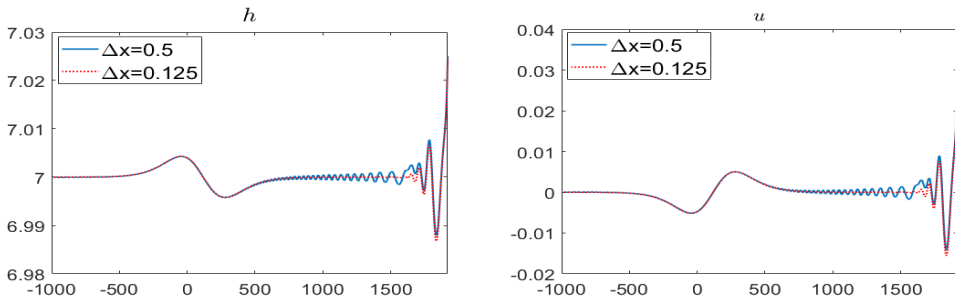


FIGURE 3. Wave-wake produced by collision of a pair of co-moving solitons at two different resolutions. Left (right) panel: height (velocity) field.

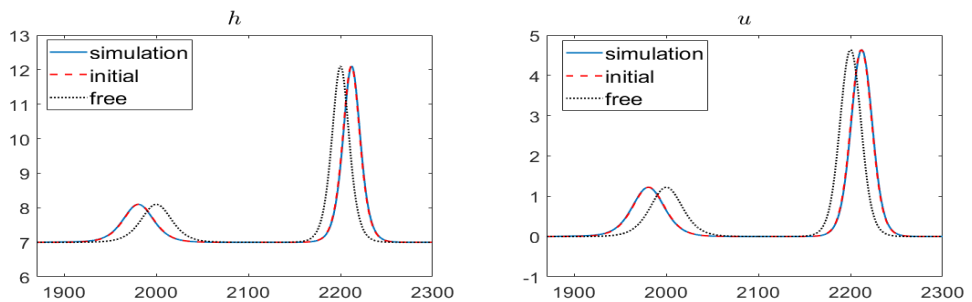


FIGURE 4. Initial data (dashed) for each soliton superimposed onto their final shapes (solid) at $t = 200$, and their respective positions in the case of free propagation with the same time lag (dotted). Left (right) panel: height (velocity) field.

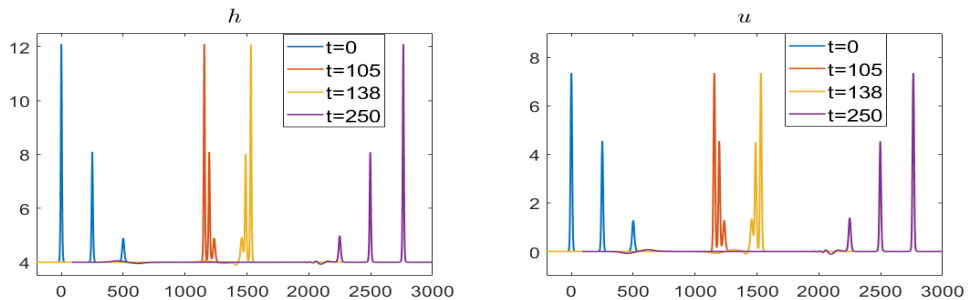


FIGURE 5. Triple collision of three co-moving solitons with $h_{max} = 12.1, 8.1, 4.9$, respectively, $H = 4$. Left (right) panel: height (velocity) field.

low-amplitude gravity waves (not shown). We, however, can choose the parameters of the initial solitons in a way that they experience a simultaneous triple collision, coalescing at some moment. In this case, which to our knowledge was not reported in the literature, the solitons also fully recover their initial form and steady motion, as follows from Fig. 5. The L_2 norms of the system, respectively, are 25.5145 at $t = 0$, and 25.5191 at $t = 250$, the quite negligible difference giving the idea of the smallness of magnitude of the wave-tail produced by the collision. Similar to those of Fig. 4 comparisons are presented in Fig. 6, and show that the highest-amplitude soliton decelerates, while two other accelerate during the impact.

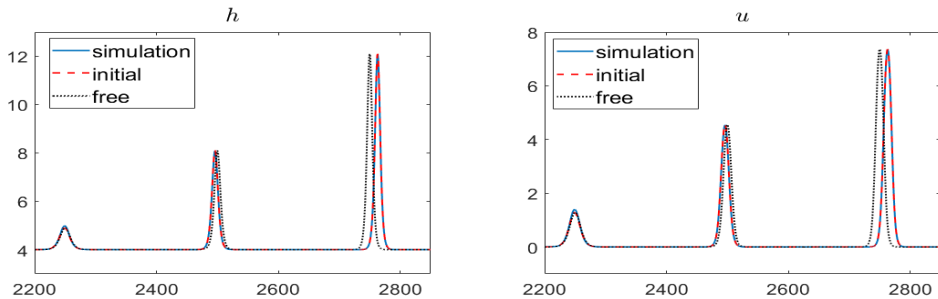


FIGURE 6. Initial data (dashed) for each soliton superimposed onto their calculated shapes (solid) at $t = 250$, and their respective positions in the case of free propagation with the same time lag (dotted). Left (right) panel: height (velocity) field.

3.1.2. Collisions of counter-propagating solitons, and of a soliton with a wall

We now test frontal collisions of two solitons. The results of one of such experiments are presented in Fig. 7, and confirm, albeit with higher resolution, those obtained earlier (Mirie & Su 1982; Dutykh *et al.* 2013; Mitsotakis *et al.* 2017). As seen in the Figure, the counter-propagating solitons recover their form and steady motion, as follows from Fig. 8 but the collision produces pronounced finite-amplitude wave-tails which are left in the wake of each soliton. In this case the existence of the wake was also proven analytically (Byatt-Smith 1988). The energy of the wakes comes from diminishing soliton amplitudes, and as a consequence of the speed, of the re-emerging solitons, which later gradually detach from the wake. As in the case of co-moving solitons, during the collision process the speed of the solitons momentarily changes, both soliton decelerating, as follows from Fig. 6.

A similar process is observed when a soliton hits a rigid wall: it recovers its form, but leaves a pronounced wave-tail in its wake after collision, see Fig. 9. In fact, a collision of two counter-propagating equal-height solitons is totally symmetric with respect to reflections $x \rightarrow -x$, if the origin is placed at the point of encounter, so collision with the wall represents its “half”, as was already noticed in (Mirie & Su 1982).

3.2. Emergence of multi-soliton configurations from localized initial conditions

We finally check whether localized initial conditions give rise a sequence of solitons, like it is the case for KdV solitons. We tested different initial distributions of h , with zero initial u . The overall result is that multi-soliton configurations do emerge, accompanied by a small-amplitude wave tails, but the number of solitons in each direction is conditioned by the shape and amplitude of the initial perturbation. We present an example of a simulation with a symmetric “flat-bump” producing sequences of 4 solitons at each of its sides in Fig. 10. Remarkably, the wave wake behind the soliton system is pulsating in this particular case. For example, for an initial Gaussian disturbance, by increasing its amplitude we observed from one to four solitons to emerge (not shown).

3.3. Interaction of solitons with topographic obstacles

Next, we investigated interactions of solitons with topographic obstacles: localized bumps, or dips, and escarpments. The results are presented in Figs. 11, 12 and show that soliton keeps its coherence passing over the first two, leaving only a detaching wave-train behind, while mounting an escarpment it generates a trailing smaller-amplitude soliton, a behavior observed in laboratory, and early numerical experiments by Seabra-Santos *et al.* (1987). This is not the case of descending escarpment, where only a wave-wake is produced. These results can be qualitatively understood in view of those on initial-value problem. As follows from (2.2), the amplitude and velocity of the

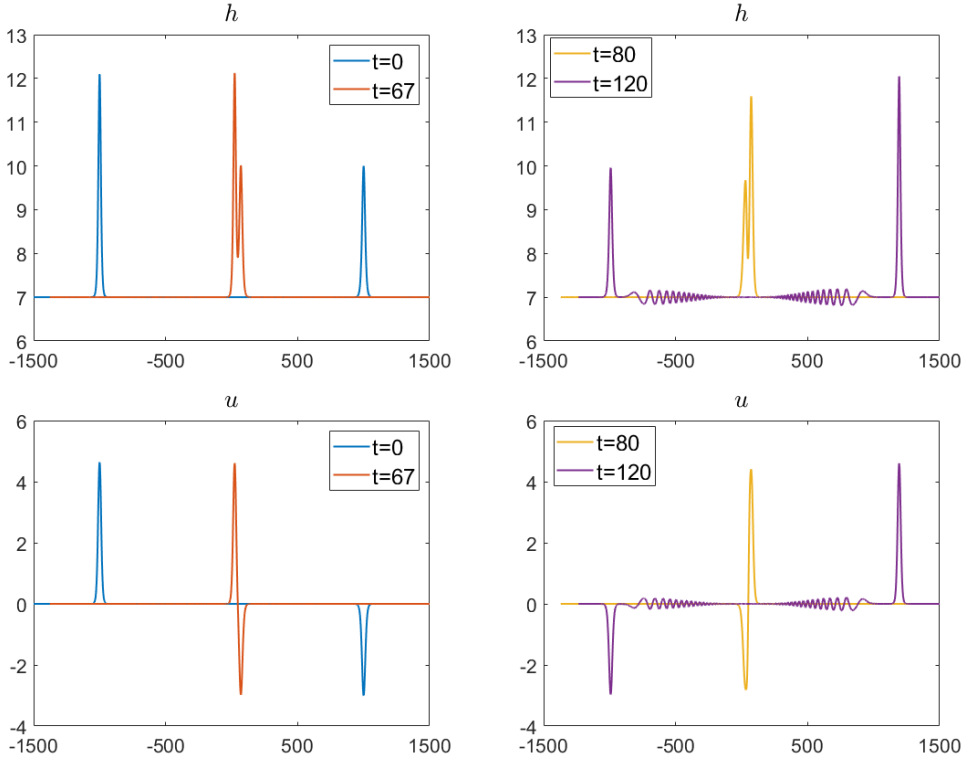


FIGURE 7. Snapshots of a collision of two counter-propagating solitons with maximum heights, respectively $h_{max} = 12.1, 10$ for two solitons at $H = 7$. Top (bottom) row : height (velocity) field.

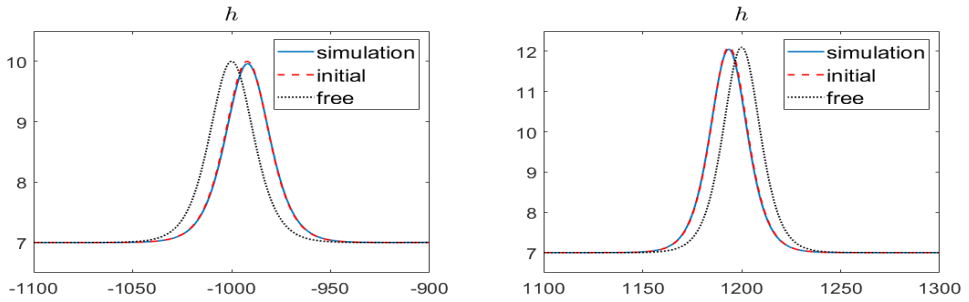


FIGURE 8. Difference between the positions and form of the left-moving (left) and right-moving (right) solitons after frontal collision of Fig. 7 (solid) with their initial forms (dashed), and with the position each soliton would have if freely propagating (dotted).

soliton increase with diminishing h_∞ . At the same time, the velocity of small-amplitude waves decreases. So mounting an escarpment the soliton should accelerate to keep this form, which is energetically impossible, so it adjusts, according to the previous results, producing a two-soliton configuration. By the same reason, descending escarpments leads to deceleration, which can be achieved by wave emission.

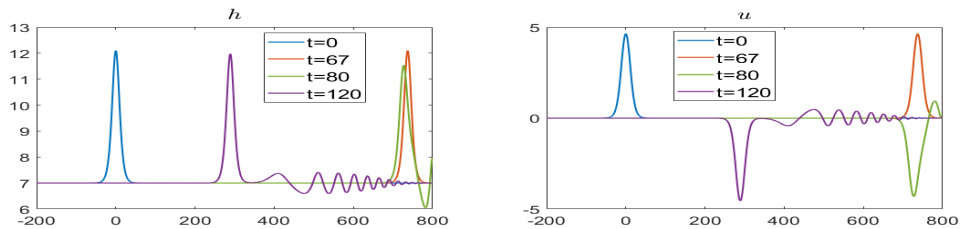


FIGURE 9. Snapshots of a collision of a soliton with a rigid wall situated at the right boundary of the simulation domain. Left (right) panel: height (velocity) field.

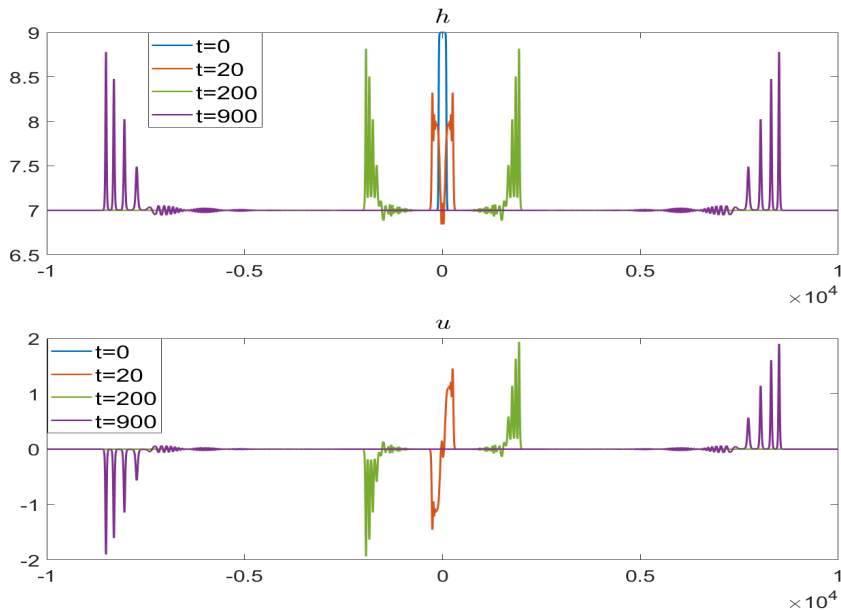


FIGURE 10. Snapshots of the evolution of an initial “flat-bump” distribution of h obtained by superposition of two tanh profiles of opposite signs, with $u \equiv 0$. Top (bottom) panel: height (velocity) field.

4. Discussion

Our simulations thus exhibit a striking resemblance in the behavior of SGN solitons with their analogs in the KdV system. This could be expected in the weak-nonlinearity (\equiv small-amplitude) limit in view of the fact that KdV is an asymptotic limit of the SGN, but is surprising for amplitudes in a range $O(1) - O(10)$. First of all, multi-soliton configurations ubiquitously arise from localized initial conditions. The collisions of co-moving solitons exhibit the same scenarios as in the KdV case, completely recovering after multiple (simultaneous or sequential) collisions, modulo small-amplitude wave-tails they leave in their wake. While such behavior was already observed in the literature for pairwise collisions, the extension to triple collisions we obtained strongly enhances similarity with the KdV system. Counter-propagating solitons also exit collisions recovering their form, but leaving a more pronounced wave wake behind. Moreover, the solitons retain their shape, emitting a wave-wake, while hitting localized topographic bumps or dips, and descending escarpments. At rising escarpments the solitons produce secondary trailing ones.

Thus, our results demonstrate an attracting character of multi-soliton configurations, and their surprising stability. We can not claim, of course, that the SGN system is completely integrable, like its descendant, the KdV equation, but ubiquity and high regularity of its multi-soliton solutions revealed by the simulations is quite remarkable.

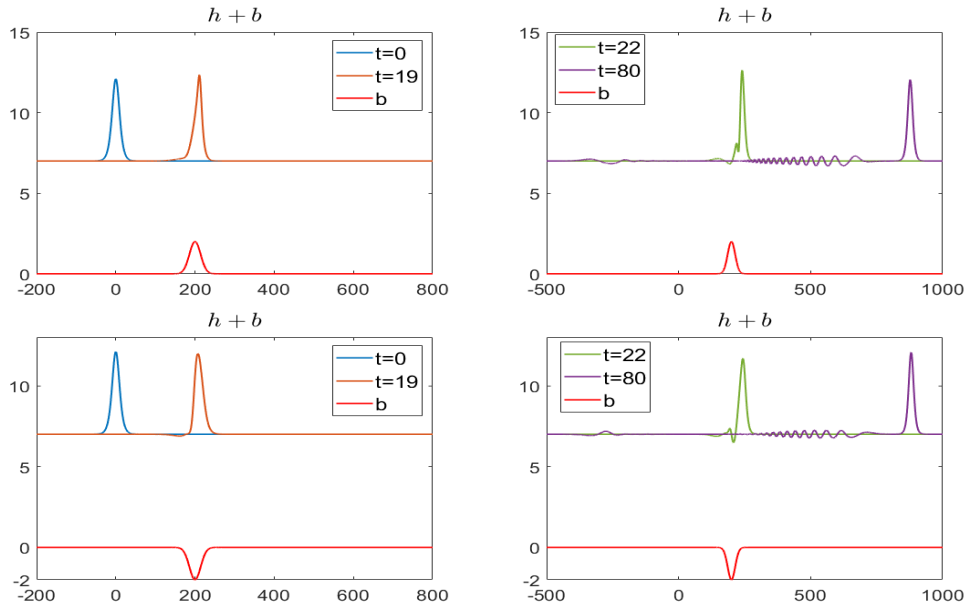


FIGURE 11. Snapshots of a height field of a soliton hitting a localized bump (top row) and a localized dip (bottom row).

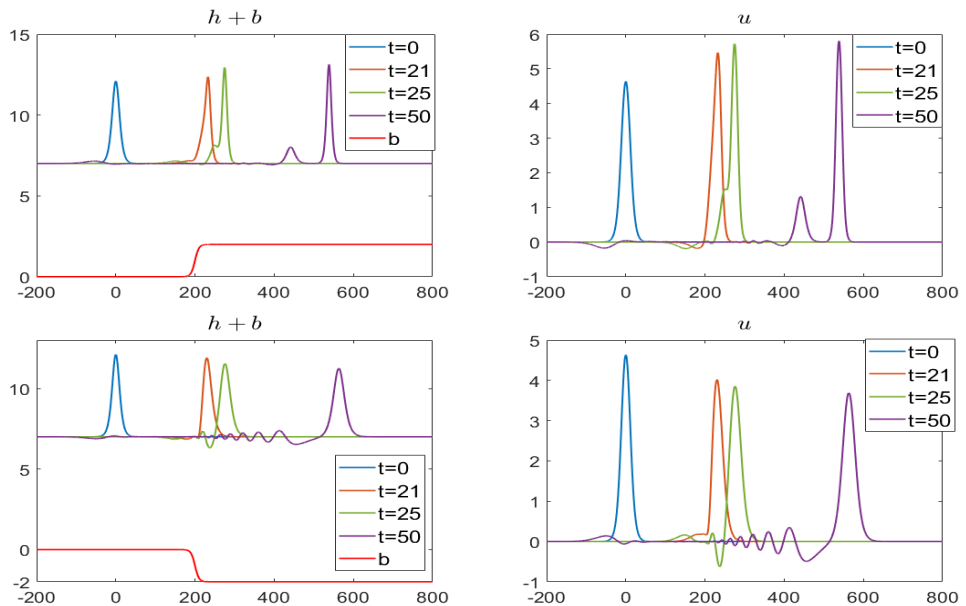


FIGURE 12. Snapshots of a height (left column) and velocity (right column) fields of a soliton hitting a rising (top row) and a descending (bottom row) escarpment of tanh shape.

REFERENCES

- BONNETON, P., BARTHELEMY, E., CHAZEL, F., CIENFUEGOS, R., LANNES, D., MARCHE, F. & TISSIER, M. 2011 Recent advances in Serre-Green Naghdi modelling for wave transformation, breaking and runup processes. *Europ. J. Mech. B/ Fluids* **30** (6), 589–597.
- BYATT-SMITH, J. G. B. 1988 The reflection of a solitary wave by a vertical wall. *J. Fluid Mech.* **197**, 503–521.

- CHENG, Y., CHERTOCK, A., HERTY, M., KURGANOV, A. & WU, T. 2019 A new approach for designing moving-water equilibria preserving schemes for the shallow water equations. *J. Sci. Comput.* **80** (1), 538–554.
- CHENG, Y. & YEH, H. 2014 Laboratory experiments on counter-propagating collisions of solitary waves. Part 1. Wave interactions. *J. Fluid Mech.* **749**, 577–596.
- CHERTOCK, A., CUI, S., KURGANOV, A., ÖZCAN, Ş. N. & TADMOR, E. 2018a Well-balanced schemes for the Euler equations with gravitation: Conservative formulation using global fluxes. *J. Comput. Phys.* **358**, 36–52.
- CHERTOCK, A., HERTY, M. & ÖZCAN, Ş. N. 2018b Well-balanced central-upwind schemes for 2×2 systems of balance laws. In *Theory, numerics and applications of hyperbolic problems. I, Springer Proc. Math. Stat.*, vol. 236, pp. 345–361. Springer, Cham.
- CHERTOCK, A., KURGANOV, A., LIU, X., LIU, Y. & WU, T. 2022 Well-balancing via flux globalization: Applications to shallow water equations with wet/dry fronts. *J. Sci. Comput.* **90** (1), paper No. 9, 21 pp.
- CRAIG, W., GUYEANNE, P., HAMMACK, J., HENDERSON, D. & SULEM, C. 2006 Solitary water wave interactions. *Phys. Fluids* **18**, paper No. 057106, 25 pp.
- DELLAR, P. J. & SALMON, R. 2005 Shallow water equations with a complete Coriolis force and topography. *Phys. Fluids* **17**, paper No. 106601, 19 pp.
- DUTYKH, D., CLAMOND, D., MILEWSKI, P. & MITSOTAKIS, D. 2013 Finite volume and pseudo-spectral schemes for the fully nonlinear 1D Serre equations. *European J. Appl. Math.* **24** (5), 761–787.
- GREEN, A. E. & NAGHDI, P. M. 1976 A derivation of equations for wave propagation in water of variable depth. *J. Fluid Mech* **78** (2), 237–246.
- KLIAKHANDLER, I. & KURGANOV, A. 2009 Quasi-Lagrangian acceleration of Eulerian methods. *Commun. Comput. Phys.* **6** (4), 743–757.
- KURGANOV, A., LIU, Y. & ZEITLIN, V. 2020 A well-balanced central-upwind scheme for the thermal rotating shallow water equations. *J. Comput. Phys.* **411**, paper No. 109414, 24 pp.
- LE MÉTAYER, O., GAVRILYUK, S. & HANK, S. 2010 A numerical scheme for the Green-Naghdi model. *J. Comput. Phys.* **229** (6), 2034–2045.
- MIRIE, R. M. & SU, C. H. 1982 Collisions between two solitary waves. Part 2. A numerical study. *J. Fluid Mech* **115**, 475–492.
- MITSOTAKIS, D., DUTYKH, D. & CARTER, J. 2017 On the nonlinear dynamics of the traveling-wave solutions of the Serre system. *Wave Motion* **70**, 166–182.
- PEARCE, J. D. & ESLER, J. G. 2010 A pseudo-spectral algorithm and test cases for the numerical solution of the two-dimensional rotating Green-Naghdi shallow water equations. *J. Comput. Phys.* **229** (20), 7594–7608.
- SEABRA-SANTOS, F. J., RENOARD, D. P. & TEMPERVILLE, A. 1987 Numerical and experimental study of the transformation of a solitary wave over a shelf or isolated obstacle. *J. Fluid Mech* **176**, 117–134.
- SERRE, F. 1953 Contribution à l'étude des écoulements permanents et variables dans les canaux. *La Houille Blanche* **39** (6), 830–872.
- SU, C. H. & GARDNER, C. S. 1969 Korteweg-de Vries equation and generalizations. III. Derivation of the Korteweg-de Vries equation and Burgers equation. *J. Math. Phys.* **10**, 536–539.
- ZABUSKY, N. J. & KRUSKAL, M. D. 1965 Interaction of “solitons” in collisionless plasma and the recurrence of initial states. *Phys. Rev. Lett.* **15** (6), 240–243.